

Acidities of Radical Anions ($pK_{\text{HA}^{\cdot-}}$) Derived from Nitro-Substituted Aromatic Weak Acids and the Formation of Radical Dianions

Yongyu Zhao and Frederick G. Bordwell*

Department of Chemistry, Northwestern University, 2145 Sheridan Road, Evanston, Illinois 60208-3113

Received August 21, 1995

A simple method has been devised for measuring the equilibrium acidities in DMSO of radical anions by using the equation $pK_{\text{HA}^{\cdot-}} = pK_{\text{HA}} + 16.8[E_{\text{rd}}(\text{HA}) - E_{\text{rd}}(\text{A}^{\cdot-})]$, which is based on a thermodynamic cycle. The acidities of 24 nitro-substituted aromatic radical anions have been measured in this way. The reversible reduction potentials to form the radical anions and those of their conjugate bases to form the radical dianions were obtained by cyclic voltammetry. The points for the irreversible $E_{\text{rd}}(\text{HA})$ values for 6 nitroaromatic compounds were found to fit on or close to the line of a plot of $E_{\text{rd}}(\text{HA})$ vs σ_{p}^- for the reversible $E_{\text{rd}}(\text{HA})$ values for 11 nitroaromatic compounds. The σ_{p}^- value for $p\text{-NH}_2$ was estimated to be about -1.0 from this plot. Relative radical dianion stabilization energies have been derived from the equilibrium acidities of the radical anions and the reduction potentials of the parent acids to provide an estimate of the stabilities of the radical dianions, relative to that of the $p\text{-OC}_6\text{H}_4\text{NO}_2^{\cdot-}$ radical dianion.

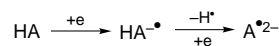
Introduction

Equilibrium acidities provide a fundamental database for assessment of the electronic and steric effects brought about by structural variations in organic molecules. The most extensive acidity scale established to date is that in DMSO, which covers the pK_{HA} range from 2 to 32 and has more than 1500 entries.¹ Thermodynamical cycles have been devised by Nicholas and Arnold to evaluate the equilibrium acidities of radical cations, $\text{HA}^{+\cdot}$,² and an equation based on one of these cycles has been used to estimate the acidities of numerous radical cations of this type in DMSO solution.³ To the best of our knowledge, no method has been devised, however, to estimate the acidities of radical anions, $\text{HA}^{\cdot-}$.

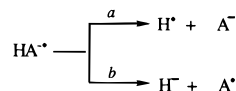
The reduction of weak acids of various types, including β -diketones, carbazole, and fluorene by alkali metals, has been shown to give radical anions and radical dianions as shown on Scheme 1,⁴ but attempts to observe such reductions electrochemically with weak acids have hitherto proved to be unsuccessful, except for $p\text{-HOC}_6\text{H}_4\text{-CH=CHCOR}$ and $p\text{-HOC}_6\text{H}_4\text{COCH=CHR}$ substrates.⁵

The bond dissociation energies for two modes of bond cleavages for $\text{HA}^{\cdot-}$ type radical anions (paths *a* and *b* in

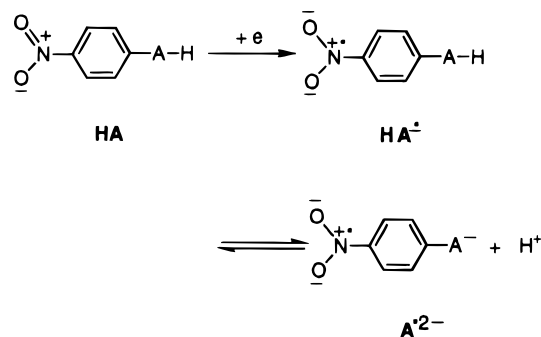
Scheme 1. Reduction of Weak Acids by Alkali Metals⁴



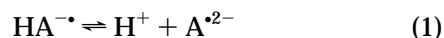
Scheme 2



Scheme 3



Scheme 2) have been estimated,⁶ but values for heterolytic cleavages of radical anions ($pK_{\text{HA}^{\cdot-}}$; eq 1) do not



appear to have been measured or estimated. In this paper we report H–O, H–N, H–C, and H–S equilibrium acidities for more than 20 radical anions of nitrobenzenoid compounds bearing acidic A–H functions (Scheme 3).

Results and Discussion

Estimates of Acidities of Radical Anions. A thermodynamic cycle has been devised (Scheme 4) that incorporates the equilibrium acidity of the parent acid,

* Abstract published in *Advance ACS Abstracts*, February 1, 1996.
(1) Bordwell, F. G. *Acc. Chem. Res.* **1988**, *21*, 456. A complete pK_{HA} list is in preparation.

(2) Nicholas, A. M. d.; Arnold, D. R. *Can. J. Chem.* **1982**, *60*, 2165–2179.

(3) (a) Bordwell, F. G.; Bausch, M. J. *J. Am. Chem. Soc.* **1986**, *108*, 2473–2474. (b) Bordwell, F. G.; Cheng, J.-P.; Bausch, M. J. *J. Am. Chem. Soc.* **1988**, *110*, 2867–2872. (c) Bordwell, F. G.; Cheng, J.-P.; Bausch, M. J. *J. Am. Chem. Soc.* **1988**, *110*, 2872–2877. (d) Bordwell, F. G.; Cheng, J.-P.; Bausch, M. J.; Bares, J. E. *J. Phys. Org. Chem.* **1988**, *1*, 209–223. (e) Bordwell, F. G.; Bausch, M. J.; Branca, J. C.; Harrelson, J. A., Jr. *J. Phys. Org. Chem.* **1988**, *1*, 225–241. (f) Bordwell, F. G.; Cheng, J.-P.; Seyedrezai, S. E.; Wilson, C. A. *J. Am. Chem. Soc.* **1988**, *110*, 8178–8183. (g) Bordwell, F. G.; Cheng, J.-P. *J. Am. Chem. Soc.* **1989**, *111*, 1792–1795. (h) Bordwell, F. G.; Cheng, J.-P. *J. Am. Chem. Soc.* **1991**, *113*, 1736–1743. (i) Bordwell, F. G.; Satish, A. V. *J. Am. Chem. Soc.* **1992**, *114*, 10173–10176. (j) Bordwell, F. G.; Zhang, X.-M.; Cheng, J.-P. *J. Org. Chem.* **1993**, *58*, 6410–6416.

(4) (a) van Willigen, H.; Weissmann, S. I. *Mol. Phys.* **1966**, *11*, 175. (b) Bauld, N. L.; Zoeller, J. H. *Tetrahedron Lett.* **1967**, 885.

(5) Martre, A. M.; Simonet, J. *J. Electroanal. Chem.* **1979**, *97*, 287–291.

(6) Zhang X.-M.; Bordwell, F. G. *J. Am. Chem. Soc.* **1994**, *115*, 904–908 and references cited therein.

(7) Jensen, B. S.; Parker, V. D. *J. Chem. Soc., Chem. Commun.* **1974**, (10), 367–368.

(8) Hansch, C.; Leo, A.; Taft, R. W. *Chem. Rev.* **1991**, *91*, 165.

Scheme 4

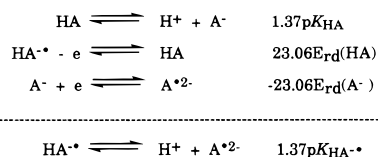


Table 1. Estimates of the Equilibrium Acidities of Radical Anions Derived from Nitro-Substituted Aromatic Weak Acids in DMSO

compound	$\text{p}K_{\text{HA}}^a$	$E_{\text{rd}}^-(\text{HA})^m$	$E_{\text{rd}}^-(\text{A}^-)^q$	$\text{p}K_{\text{HA}^{\bullet-}}^r$
1. <i>p</i> -NO ₂ C ₆ H ₄ OH	10.8 ^b	-1.609	-2.215	21.0
2. <i>m</i> -NO ₂ C ₆ H ₄ OH	14.4 ^b	-1.573	-1.873	19.4
3. <i>p</i> -Cl-2,6-(NO ₂) ₂ C ₆ H ₂ OH	3.6 ^c	-0.898	-1.620	15.7
4. 2,4-(NO ₂) ₂ C ₆ H ₃ OH	5.1 ^c	-0.981 ⁿ	-1.818	19.8
5. 2,4-dinitronaphthol	2.1 ^c	-0.871 ⁿ	-1.764	17.1
6. <i>p</i> -NO ₂ C ₆ H ₄ COOH	9.0 ^c	-1.281	-1.554	13.6
7. 3,5-(NO ₂) ₂ C ₆ H ₃ COOH	7.3 ^c	-1.135	-1.336	10.7
8. <i>cis-m</i> -NO ₂ C ₆ H ₄ CH=NOH	17.7 ^d	-1.462 ^o	-1.605	20.1
9. <i>trans-m</i> -NO ₂ C ₆ H ₄ CH=NOH	17.6 ^d	-1.460 ^o	-1.631	20.5
10. <i>cis-p</i> -NO ₂ C ₆ H ₄ CH=NOH	17.0 ^d	-1.393 ^o	-1.658	21.5
11. <i>p</i> -NO ₂ C ₆ H ₄ SH	5.5 ^e	-1.284	-1.877	15.5
12. <i>p</i> -NO ₂ C ₆ H ₄ NHPh	16.9 ^f	-1.658 ⁿ	-2.209	26.1
13. <i>p</i> -NO ₂ C ₆ H ₄ NHCOMe	17.6 ^g	-1.572 ^o	-1.869	22.6
14. 2,4-(NO ₂) ₂ C ₆ H ₃ NH ₂	15.9 ^c	-1.416 ^o	-1.676	20.3
15. 2-nitrofluorene	17.0 ^f	-1.491 ^o	-1.949	24.7
16. 2,7-dinitrofluorene	12.2 ^h	-1.378 ⁿ	-1.715	17.9
17. <i>p</i> -NO ₂ C ₆ H ₄ CH ₂ CN	12.3 ^c	-1.479 ^{n,p}	-2.151	23.4
18. <i>m</i> -NO ₂ C ₆ H ₄ CH ₂ CN	18.1 ^c	-1.445 ^o	-1.792	23.9
19. <i>m</i> -NO ₂ C ₆ H ₄ CH ₂ NO ₂	10.0 ^j	-1.429	-1.624	13.3
20. <i>p</i> -NO ₂ C ₆ H ₄ CH(Me)NO ₂	10.3 ^j	-1.396	-1.659	14.7
21. <i>m</i> -NO ₂ C ₆ H ₄ CH(Me)NO ₂	11.5 ^j	-1.420 ^o	-1.635	15.1
22. 3,5-(NO ₂) ₂ C ₆ H ₃ CH(Me)NO ₂	9.9 ^j	-1.167 ^o	-1.392	13.7
23. <i>p</i> -NO ₂ C ₆ H ₄ CH ₂ P ⁺ Ph ₃ Br ⁻	11.4 ^k	-1.419 ^{n,p}	-1.883	19.2
24. <i>p</i> -NO ₂ C ₆ H ₄ C(Ph)=NCH ₂ CO ₂ Et	16.7 ^l	-1.397 ^o	-1.784	23.2

^a In $\text{p}K_{\text{HA}}$ units; equilibrium acidities were measured in DMSO solution. ^b Reference 3h. ^c Reference 1. ^d Reference 9. ^e Reference 10. ^f Reference 6. ^g Reference 11. ^h Measured by A. V. Satish. ⁱ Reference 12. ^j Reference 13. ^k Reference 14. ^l Measured by X.-M. Zhang. ^m In volts; irreversible reduction potentials of the neutral compounds were measured in DMSO solution and referenced to ferrocenium/ferrocene couple. ⁿ Partially reversible reduction potential. ^o Reversible reduction potential. ^p Sweep rate: 500 mV/s. ^q In volts; reversible reduction potentials were measured. ^r In $\text{p}K_{\text{HA}}$ units; estimated by eq 2.

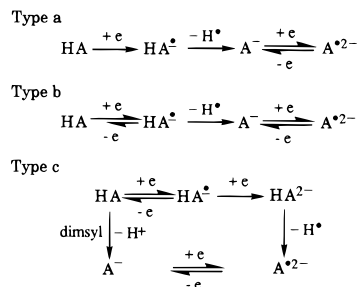
its reduction potential, $E_{\text{rd}}(\text{HA})$, and that of its conjugate base, $E_{\text{rd}}(\text{A}^-)$, in order to evaluate the equilibrium acidity, $\text{p}K_{\text{HA}^{\bullet-}}$, of a radical anion [eq 2; the constant 16.8 (23.06/1.37) converts volts to $\text{p}K$ units].

$$\text{p}K_{\text{HA}^{\bullet-}} = \text{p}K_{\text{HA}} + 16.8[E_{\text{rd}}(\text{HA}) - E_{\text{rd}}(\text{A}^-)] \quad (2)$$

The $\text{p}K_{\text{HA}^{\bullet-}}$ values estimated by eq 2 for 24 nitro aromatic radical anions, together with the $\text{p}K_{\text{HA}}$, $E_{\text{rd}}(\text{HA})$, and $E_{\text{rd}}(\text{A}^-)$ values are listed in Table 1.

Classification of Nitro-Substituted Aromatic Acids Based on the Relative Stabilities of the Corresponding Radical Anions. The nitro group is one of the strongest of the common electron-withdrawing groups and is one of the most adept in accepting one electron to form the corresponding radical anion. For example, nitrobenzene is readily reduced electrochemically to the corresponding radical anion and even to a dianion in DMF.⁷ The reversible reduction potential for nitroben-

Scheme 5



zene in DMSO is -1.510 V. Introduction of an electron-withdrawing group into the para position of nitrobenzene shifts the potential to a more positive position by stabilizing the radical anion being formed, and introduction of an electron-donating group has the opposite effect. For example, the reversible reduction potentials for *p*-NO₂-C₆H₄CO₂Et and *p*-NO₂-C₆H₄OPh are -1.287 and -1.533 V, respectively.

Our electrochemical studies of nitro-substituted aromatic acids show that about half of the radical anions generated on the electrode in Table 1 are stable enough on the cyclic voltammetric (CV) time scale (sweep rate 100 mV/s) to give reversible reduction potentials, whereas the other half are less stable and give partially reversible or irreversible potentials. The radical anions formed can be classified into three types according to their relative kinetic stabilities on the electrode, as shown in Scheme 5.

The cyclic voltammograms observed for the reduction potentials can be correlated to some extent with the nature of the radical anions being formed. Radical anions following type a (irreversible) behavior are markedly unstable and rapidly undergo loss of a hydrogen atom to form a monoanion (A^-) which is then reduced reversibly to give a radical dianion ($\text{A}^{\bullet-}$).¹⁵ For example, *p*-nitrobenzoic acid (entry 6 in Table 1) gives two reduction potentials (Figure 1). The first (irreversible) peak (pc1) is due to the reduction of the parent acid to give the radical anion, and the second (reversible) pair of peaks (pc2 and pa2) is formed due to the reduction of the decay product (A^-) to give the radical dianion ($\text{A}^{\bullet-}$). This reaction sequence is shown in Scheme 6.

If the reaction sequence shown in Scheme 6 is correct, it should be possible to obtain the radical dianion by simply adding potassium dimsyl ($\text{CH}_3\text{SOCH}_2\text{-K}^+$) in DMSO to neutralize the acid prior to carrying out the reduction. The sequence of reactions then becomes that shown in Scheme 7.

The CV obtained under these conditions (Figure 2) shows only the pair of reversible peaks for the formation of the radical dianion and its reoxidation to the anion.

The corresponding radical anions derived from the nitro-substituted aromatic acids of type b are more stable than those derived from type a, but not so stable as those derived from type c (vide infra), and often give partially reversible potentials. For example, both 1-(*m*-nitrophenyl)-1-nitroethane (entry 21) and 4-nitrodiphenylamine (entry 12) belong to this category. The difference between their CVs lies in that the initial reversible potential for entry 21 was accompanied by a pair of small broad

(9) Bordwell, F. G.; Ji, G.-Z. *J. Org. Chem.* **1992**, 57, 3019.

(10) Bordwell, F. G.; Zhang, X.-M.; Satish, A. V.; Cheng, J.-P. *J. Am. Chem. Soc.* **1994**, 116, 6605-6610.

(11) Cheng, J.-P.; Zhao, Y. *Tetrahedron* **1993**, 49, 5267-5276.

(12) Keefe, J. R.; Morey, J.; Palmer, C. A.; Lee, J. C. *J. Am. Chem. Soc.* **1979**, 101, 1295-1297.

(13) Bordwell, F. G.; Zhao, Y. *J. Org. Chem.* **1995**, 60, 6348.

(14) Zhao, Y. Ph.D. Dissertation, Nankai University, 1994, Tianjin, P. R. China.

(15) We are indebted to a referee who pointed out that the protonation of the radical anion by the unreacted starting material may also account for the formation of the corresponding anion.

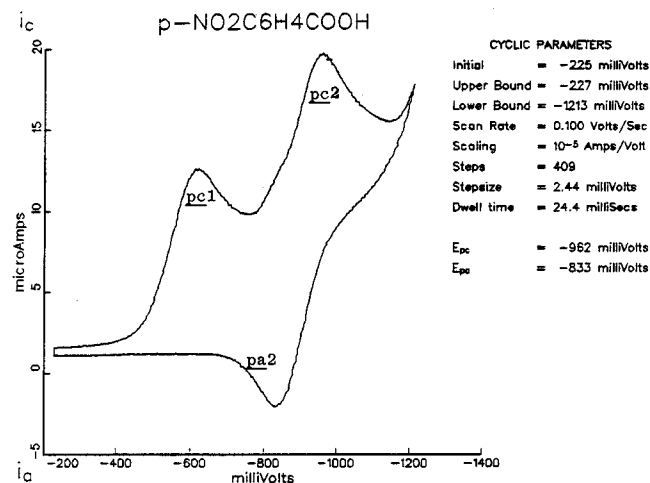
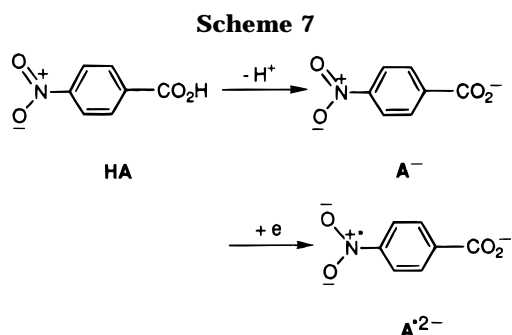
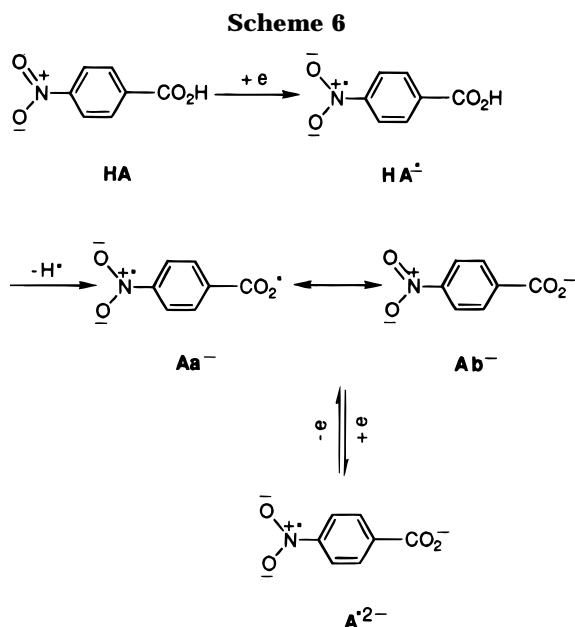


Figure 1. Reduction potential of 4-nitrobenzoic acid in DMSO [the first irreversible peak (pc1)], referenced to Ag/AgI couple. The scan rate was 100 mV/s, and Et₄N⁺BF₄⁻ was the supporting electrolyte.



shoulders (Figure 3), indicating that the corresponding radical anion was quite stable and that only a small portion of the radical anions decompose to give the anion, whereas for entry 12 the initial partially reversible potential was accompanied by a pair of prominent peaks (Figure 4), showing that a substantial number of radical anions had undergone decay to form the anion.

The radical anions derived from type c were the most stable among these three types and usually did not decay to form the corresponding anions. In the CV (Figure 5)

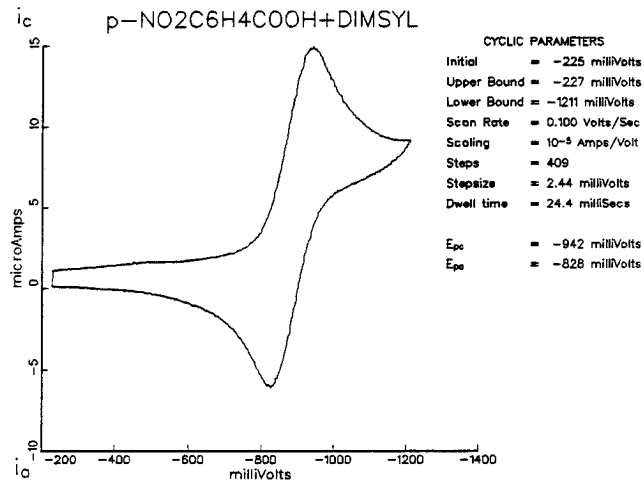


Figure 2. Reduction potential of the conjugate base of 4-nitrobenzoic acid in DMSO, referenced to Ag/AgI couple. The scan rate was 100 mV/s, and Et₄N⁺BF₄⁻ was the supporting electrolyte.

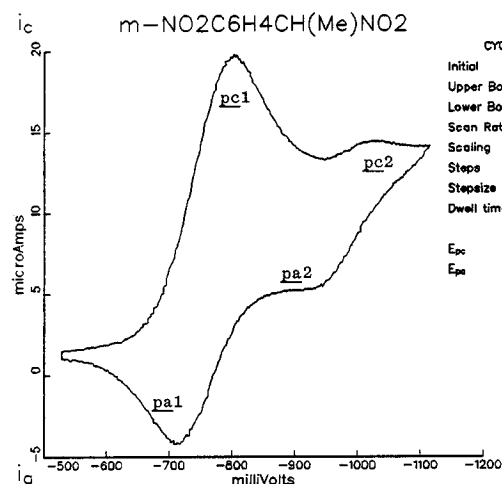


Figure 3. Reduction potential of 1-(3-nitrophenyl)-1-nitroethane in DMSO, referenced to Ag/AgI couple. The scan rate was 100 mV/s, and Et₄N⁺BF₄⁻ was the supporting electrolyte.

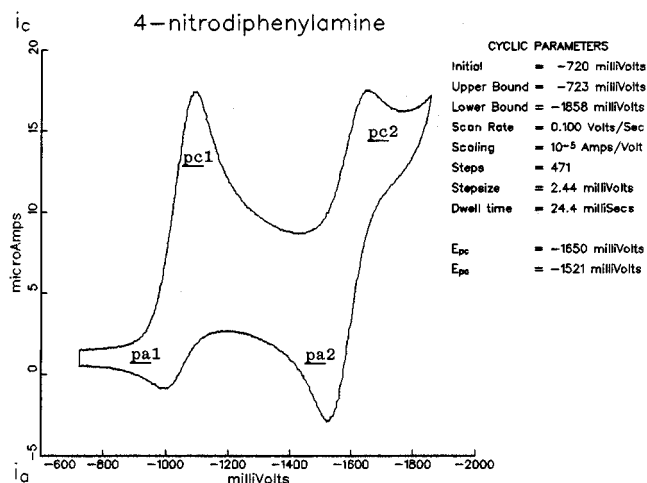


Figure 4. Reduction potential of 4-nitrodiphenylamine in DMSO, referenced to Ag/AgI couple. The scan rate was 100 mV/s, and Et₄N⁺BF₄⁻ was the supporting electrolyte.

of *m*-nitrophenylacetonitrile (entry 18), for example, no cathodic peak (pc2) due to the reduction of the anion was observed in negative-going sweep. But the CV did have

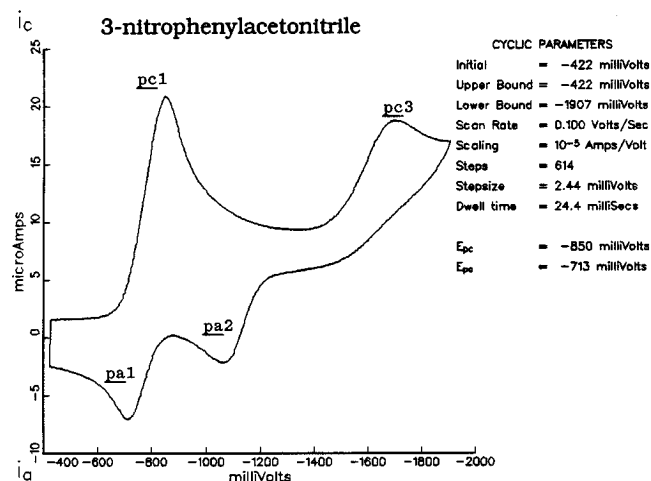


Figure 5. Reduction potential of 3-nitrophenylacetonitrile in DMSO, referenced to Ag/AgI couple. The scan rate was 100 mV/s, and $\text{Et}_4\text{N}^+\text{BF}_4^-$ was the supporting electrolyte.

a new cathodic peak (pc3) at a more negative potential, which can be attributed to the formation of the dianion (vide infra). In the positive-going sweep, in addition to the anodic peak (pa1) for the radical anion to be reoxidized to the neutral acid, there is a second anodic peak (pa2) at a more negative potential. This peak can be assigned to the oxidation of the radical dianion to the anion because (a) the decrease of peak height of pc1 was accompanied by the appearance of a new cathodic peak (pc2) at a potential between pc1 and pc3 and by the increase of peak height of pa2 after the addition of a few drops of dimsyl and (b) only pc2 and pa2 peaks remained when an equivalent of dimsyl was added.

The radical dianion accounting for the appearance of the pa2 before the addition of dimsyl was presumably generated by the homolytic cleavage of the acidic H-A bond in the dianion, HA^{2-} , by loss of a hydrogen atom, i.e., $\text{HA}^{2-} \rightleftharpoons \text{H}^\bullet + \text{A}^{2-}$.

It should be noted that the boundaries between these three types of nitro-substituted aromatic acids are not clear-cut. For example, the reduction potential for *p*-nitrophenylacetonitrile was not reversible at the voltage sweep rate of 100 mV/s, but it was partially reversible when the sweep rate was increased to 500 mV/s. For 1-(*m*-nitrophenyl)-1-nitroethane, which has been given as an example of type b behavior (vide supra), both the small peaks (pc2 and pa2) for the A^-/A^{2-} couple and the more cathodic peak (pc3) due to the formation of the dianion were observed when the voltage was swept to -1.800 V.

Comparison of Irreversible and Partially Reversible Reduction Potentials with Reversible Reduction Potentials. For accurate estimates of pK_{HA^-} values by eq 2, thermodynamically reversible reduction potentials should be used. The values given in Table 1 for the $E_{\text{rd}}(\text{A}^-)$ values are reversible, but about half the $E_{\text{rd}}(\text{HA})$ values in Table 1 are partially reversible or irreversible. In order to estimate the uncertainties of the irreversible or partially reversible reduction potentials, the reversible reduction potentials [$E_{\text{rd}}(\text{HA})$] for 11 para-substituted nitrobenzenes (Table 2) were plotted versus σ_p^- constants,⁸ and a reasonably good line ($r = 0.989$) was obtained (Figure 6). The theoretically reversible reduction potentials for six para-substituted nitrobenzene were calculated using the equation obtained by regression analysis. The results are compared in Table 3 with the

Table 2. Reduction Potentials for *Para*-Substituted Nitrobenzenes ($p\text{-GC}_6\text{H}_4\text{NO}_2$) and σ_p^- Values for the Corresponding Substituents

no.	G	$E_{\text{rd}}(\text{HA})^a$	$\sigma_p^-^b$	no.	G	$E_{\text{rd}}(\text{HA})^a$	$\sigma_p^-^b$
1	Et	-1.560	-0.19	7	COOEt	-1.287	0.75
2	Me	-1.560	-0.17	8	COMe	-1.263	0.84
3	Oph	-1.533	-0.10	9	CN	-1.206	1.00
4	H	-1.510	(0.0)	10	CHO	-1.203	1.03
5	Br	-1.409	0.25	11	SO ₂ Me	-1.238	1.13
6	CONH ₂	-1.361	0.61				

^a In volts, reversible reduction potential measured in DMSO solution by cyclic voltammetry and referenced to ferrocenium/ferrocene (Fc^+/Fc) couple. ^b Data from ref 8.

$$E_{\text{rd}}(\text{HA}) = -1.5046 + 0.27579 \sigma_p^- \quad R = 0.989$$

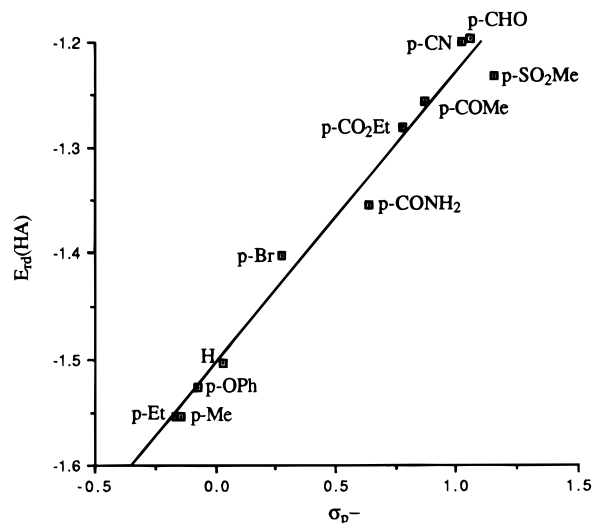


Figure 6. Plot of the reversible reduction potentials [$E_{\text{rd}}(\text{HA})$] for 4- $\text{GC}_6\text{H}_4\text{NO}_2$ versus Hammett σ_p^- constants.

Table 3. Comparison of Experimental Values [$E_{\text{rd}}(\text{HA})_{\text{exp}}$] with Calculated Values [$E_{\text{rd}}(\text{HA})_{\text{cal}}$] by a Hammett Plot

	G					
	COOH	OH	CH ₂ CN	NHPh	NHCOMe	NH ₂
$\sigma_p^-^a$	0.77	-0.37	0.11	-0.29	-0.46	-0.15
$E_{\text{rd}}(\text{HA})_{\text{cal}}^b$	-1.292	-1.607	-1.474	-1.585	-1.631	-1.546
$E_{\text{rd}}(\text{HA})_{\text{exp}}^c$	-1.281	-1.609	-1.479 ^e	-1.658 ^f	-1.572 ^g	-1.792 ^g
$\Delta E_{\text{rd}}(\text{HA})^d$	0.011	-0.002	-0.005	-0.027	0.059	-0.246

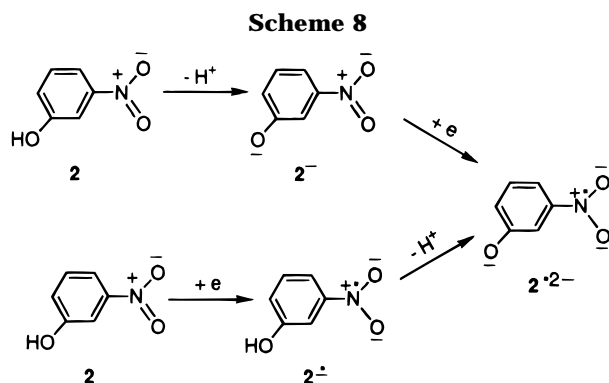
^a Data from ref 8. ^b In volts, calculated from the least-squares line in Figure 6 by using $E_{\text{rd}}(\text{HA}) = -1.5046 + 0.27579 \sigma_p^-$. ^c In volts, irreversible reduction potential measured in DMSO solution by cyclic voltammetry unless otherwise noted and referenced to ferrocenium/ferrocene (Fc^+/Fc) couple. ^d In volts, calculated by using $\Delta E_{\text{rd}}(\text{HA}) = E_{\text{rd}}(\text{HA})_{\text{exp}} - E_{\text{rd}}(\text{HA})_{\text{cal}}$. ^e In volts, partially reversible reduction potential, sweep rate: 500 mV/s. ^f In volts, partially reversible reduction potential. ^g In volts, reversible reduction potential.

corresponding experimental data. Examination of the data listed in Table 3 shows that the experimental data for the para substituents are in good agreement with the calculated data except for the *p*-NH₂ group. The *p*-NH₂ group is a much better electron donor than either the *p*-NHPh or *p*-NHCOMe group, which have been assigned σ_p^- values of -0.29 and -0.46 , respectively. The -0.15 value assigned to σ_p^- for the *p*-NH₂ group⁸ must be in error. From the slope of the line in Figure 6 and the reduction potential for the *p*-NH₂ group, we estimate that σ_p^- for the *p*-NH₂ group is about -1.0 . The larger $\Delta E_{\text{rd}}(\text{HA})$ values for the *p*-NHPh or *p*-NHCOMe groups than those for *p*-CO₂H, *p*-OH, and *p*-CH₂CN groups in Table

Table 4. Relative Radical Dianion Stabilization Energies (RRDSE) for Representative Nitro-Substituted Aromatic Weak Acids in DMSO

compound	ΔpK_{HA}^a	$\Delta E_{rd}^-(HA)^a$	$\Delta E_{rd}^-(A^-)^a$	$\Delta pK_{HA\cdot}^a$	RRDSE ^b
1. <i>p</i> -NO ₂ C ₆ H ₄ OH	(0.0)	(0.0)	(0.0)	(0.0)	(0.0)
2. <i>m</i> -NO ₂ C ₆ H ₄ OH	4.9	0.8	7.9	-2.2	3.0
3. <i>p</i> -NO ₂ C ₆ H ₄ CH=NOH	8.5	5.0	12.8	0.7	4.3
4. <i>p</i> -NO ₂ C ₆ H ₄ SH	-7.3	7.5	7.8	-7.5	15.0
5. <i>p</i> -NO ₂ C ₆ H ₄ NHPh	8.4	-1.1	0.1	7.2	-8.3
6. <i>p</i> -NO ₂ C ₆ H ₄ NHCOMe	9.3	0.9	8.0	2.2	-1.1
7. <i>p</i> -NO ₂ C ₆ H ₄ CH ₂ CN	2.1	3.0	1.5	3.6	-0.6
8. <i>m</i> -NO ₂ C ₆ H ₄ CH ₂ CN	10.0	3.8	9.8	4.0	-0.2
9. <i>m</i> -NO ₂ C ₆ H ₄ CH ₂ NO ₂	-1.1	4.2	13.6	-10.5	14.7
10. <i>p</i> -NO ₂ C ₆ H ₄ CH ₂ P ⁺ Ph ₃ Br ⁻	0.8	4.4	7.7	-2.5	6.9
11. 2-nitrofluorene	8.5	2.7	6.1	5.1	2.4

^a In kcal/mol, calculated by using data listed in Table 1. ^b In kcal/mol, calculated by using the equation $RRDSE = \Delta E_{rd}(HA) - \Delta pK_{HA\cdot}$ or $RRDSE = \Delta E_{rd}(A^-) - \Delta pK_{HA}$.



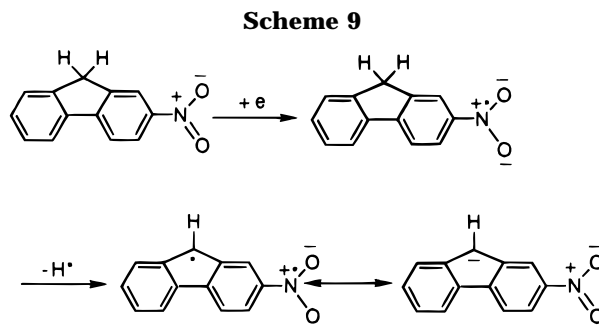
3 make the assigned σ_p^- values for these groups⁸ also suspect. In other papers we have presented evidence to indicate that irreversible redox potentials usually do not differ by more than 50–100 mV from reversible potentials. The close fit for most of the irreversible potentials with the reversible potentials in Figure 6 add further evidence on this score.

Relative Radical Dianion Stabilization Energies (RRDSE). In considering the effects of structural changes on solution pK_{HA} values, $HA \rightleftharpoons H^+ + A^-$, one can relate the acidity changes to effects on A^- anion stabilities in the medium used because the effects on the undissociated acid stabilities are usually small. In considering the effects of structural changes on solution $pK_{HA\cdot}$ values of radical cations, $HA^{\cdot+} \rightleftharpoons H^+ + A^{\cdot+}$, one can relate the acidity changes to effects on $HA^{\cdot+}$ stabilities because the effects on $A^{\cdot+}$ stabilities are usually small.³ But in considering the effects of structural changes on $pK_{HA\cdot}$ values of radical anions, $HA^{\cdot-} \rightleftharpoons H^+ + A^{2-}$, it is necessary to evaluate the effects on both $HA^{\cdot-}$ and A^{2-} because both are negatively charged. Here a lower $pK_{HA\cdot}$ value could mean a more stable product radical dianion and/or a less stable undissociated radical anion.

In Table 4, ΔpK_{HA} , $\Delta E_{rd}(HA)$, $\Delta E_{rd}(A^-)$ and $\Delta pK_{HA\cdot}$ values for representative nitro-substituted aromatic weak acids in DMSO, relative to the values for *p*-nitrophenol, are given. (All values have been converted to kcal/mol.)

One can visualize the formation of radical dianions from the weak acids in Table 4 as occurring either by (a) ionization of the acid (pK_{HA}) followed by reduction of the anion, $E_{rd}(A^-)$, or (b) reduction of the acid, $E_{rd}(HA)$, followed by ionization of the $HA^{\cdot-}$ radical anion. These paths are illustrated for *m*-nitrophenol (**2**) in Scheme 8.

The differences in energies brought about by combination of either of these pathways, relative to those brought



about for *p*-nitrophenol, provide a measure of the relative radical dianion stabilization energies (RRDSE) for the ten other radical dianions shown in Table 4. For example, $RRDSE = \Delta E_{rd}(A^-) - \Delta pK_{HA} = 7.9 - 4.9 = 3$ kcal for the radical dianion (**2**²⁻) for *m*-nitrophenol and the same value for the RRDSE of **2**²⁻ is obtained from $RRDSE = \Delta E_{rd}(HA) - \Delta pK_{HA\cdot}$ for *m*-nitrophenol, i.e., $0.8 - (-2.2) = 3.0$ kcal. The hydroxyl group in *p*-nitrophenol tends to destabilize the radical anions being formed by shifting the reduction potential to a more negative position. In other words, *m*-nitrophenol is easier to reduce than *p*-nitrophenol because the destabilizing effect of the *m*-hydroxy group on the radical anion being formed is smaller. In the para isomer donor resonance and electrostatic effects are both operative whereas in the meta isomer the donor effect is primarily electrostatic.

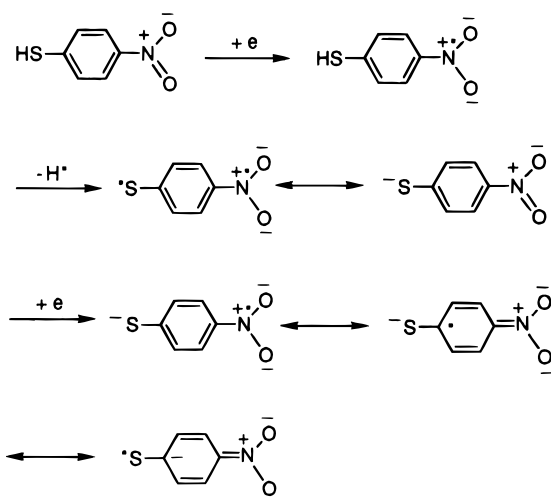
Radical dianions are inherently unstable species since they bear a double negative charge as well as an odd electron. The nitro group can exert an unusually large stabilizing effect since it can stabilize both a negative charge and an odd electron. All of the 11 entries in Table 4 contain at least one nitro group, and most contain a second electron-withdrawing group. The conjugate base of *p*-nitrotoluene cannot be further reduced under the conditions used for the compounds in Table 4, but the ability of the fluorene ring to stabilize a negative charge (Scheme 9) makes electrochemical reduction to a radical dianion feasible for 2-nitrofluorene (entry 11). Also, the introduction of the electron-withdrawing Ph₃P⁺ group into the methyl group of toluene allows the formation of the ylide radical dianion (entry 10).

The radical dianion derived from *p*-nitrothiophenol (entry 4) has the largest RRDSE in Table 4 (15 kcal) because of the strong ability of the sulfur to accommodate a negative charge and odd electron (Scheme 10). The radical dianion derived from entry 9 is almost as stable ($RRDSE = 14.7$ kcal). Here one nitro group accommodates the odd electron and each nitro group accommodates a negative charge in the radical dianion (Scheme 11).

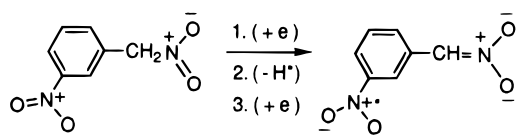
The radical dianions with nitrogen as a donor atom (entry 5 and 6) are less stable than their oxygen analogues owing to the stronger basicity of the nitrogen than the oxygen anion.

Acidities of Radical Anions. All of the radical anions in Table 1 have the odd electron attached to a nitro group. They vary in acidity from $pK_{HA\cdot} = 10.7$ for 3,5-(NO₂)₂C₆H₃OH to $pK_{HA\cdot} = 26.1$ for *p*-NO₂C₆H₄NHPh, a range of 15.7 pK_{HA} units (21 kcal), and are less acidic than their parent acids by an average of 6.8 pK_{HA} units (9.3 kcal). The weaker acidity is expected because of the negative charge on the undissociated acid, which retards the loss of a proton, and the inherent instability of the radical dianion. Structural changes that enhance the

Scheme 10



Scheme 11



acidity of the parent, such as the presence of one or two nitro groups at the 2, 4, or 6 position of phenols, as in entries in Table 1, have much less effect on the acidities of their radical anions than on the parent acids. Note, for example, that *m*-NO₂C₆H₄OH^{•-} is a stronger acid than *p*-NO₂C₆H₄OH^{•-} because the RRDSE of the meta isomer is 3 kcal greater. The RRDSE values for the radical dianion products can play an important role in determining the acidities of the radical anions. When the RRDSE values are large, as for the radical dianions derived from entries 4, 9, and 10 in Table 4, there are sizable increases in the acidities of the undissociated HA^{•-} radical anion, relative to that of the *p*-NO₂C₆H₄OH^{•-} radical anion, because the equilibrium in eq 1 (Scheme 2) will be shifted to the right. The RRDSE values are small for entries 2, 3, and 11 in Table 4, indicating that the stabilities of the radical dianions play a lesser role in determining the HA^{•-} radical dianion acidities. For entries 5, 6, 7, and 8 in Table 4 the RRDSE values are negative because the basicity of the anion moiety in the radical dianion is

greater than that of the oxide ion in the *p*-OC₆H₄NO₂^{•-} radical dianion. The marked instability of the radical dianion derived from entry 5 will have a sizable acid weakening effect on the parent HA^{•-} radical dianion acidity.

Summary and Conclusions

The nitro group is one of the strongest of the common electron-withdrawing groups and is probably the most adept in accepting one electron to form the corresponding radical anion. The radical anions derived from 24 nitro-substituted aromatic weak acids can be classified into three types according to their relative kinetic stabilities on the electrode. A reasonably good line (Figure 6; *r* = 0.989) was obtained when the reversible reduction potentials [*E*_{rd}(HA)] for 11 para-substituted nitrobenzenes were plotted versus *σ*_p⁻ constants. The good fit of the *E*_{rd}(HA) values in Figure 6 shows that our estimates of p*K*_{HA^{•-}} values using irreversible, as well as reversible, potentials are accurate. In considering the effects of structural changes on p*K*_{HA^{•-}} values of radical anions, HA^{•-} ⇌ H⁺ + A²⁻, it is necessary to evaluate the effects on both HA^{•-} and A²⁻ because both are negatively charged. A lower p*K*_{HA^{•-}} value could mean a more stable product radical dianion and/or a less stable undissociated acidic radical anion HA^{•-}. Relative radical dianion stabilization energies (RRDSE) have been derived to provide an estimate of the relative stabilities of the radical dianions relative to that of *p*-OC₆H₄NO₂^{•-}.

Experimental Section

All of the compounds studied in this paper were previously synthesized in our laboratory¹³ or purchased. The reduction potentials were measured by cyclic voltammetry (CV). The working electrode (BAS) consists of a 1.5-mm-diameter platinum disk embedded in a cobalt glass seal. It was polished with 0.05-mm Fischer polishing aluminum or cleaned with an ultrasonic instrument, rinsed with ethanol, and dried before each run. The counterelectrode was a platinum wire (BAS). The reference electrode was Ag/AgI, and the reported potentials were referenced to ferrocenium/ferrocene (Fc⁺/Fc) couple. Tetraethylammonium tetrafluoroborate was used as the supporting electrolyte. All electrochemical experiments were carried out under an argon atmosphere.

Acknowledgment. We are grateful to the National Science Foundation for support of this research.

JO951542F